Facultative protein selenation regulates redox sensitivity, adipose tissue thermogenesis, and obesity

Mark P. Jedrychowski[a,b,1], Gina Z. Lu[a,b], John Szpyt[b], Marco Mariotti[c], Ryan Garrity[a,b], Joao A. Paulo[b], Devin K. Schweppe[b], Dina Laznik-Bogoslavski[a,b], Lawrence Kazak[a,b], Michael P. Murphy[d,e], Vadim N. Gladyshev[c], Steven P. Gygi[b], Edward T. Chouchani[a,b,1], and Bruce M. Spiegelman[a,b,1]

[a]Department of Cancer Biology, Dana–Farber Cancer Institute, Boston, MA 02115; [b]Department of Cell Biology, Harvard Medical School, Boston, MA 02115; [c]Division of Genetics, Department of Medicine, Brigham and Women's Hospital and Harvard Medical School, Boston, MA 02115; [d]Medical Research Council (MRC) Mitochondrial Biology Unit, University of Cambridge, Cambridge CB20XY, United Kingdom; and [e]Department of Medicine, University of Cambridge, Cambridge CB20XY, United Kingdom

Contributed by Bruce M. Spiegelman, March 27, 2020 (sent for review January 24, 2020; reviewed by David J. Mangelsdorf and Lucia A. Seale)

Oxidation of cysteine thiols by physiological reactive oxygen species (ROS) initiates thermogenesis in brown and beige adipose tissues. Cellular selenocysteines, where sulfur is replaced with selenium, exhibit enhanced reactivity with ROS. Despite their critical roles in physiology, methods for broad and direct detection of proteogenic selenocysteines are limited. Here we developed a mass spectrometric method to interrogate incorporation of selenium into proteins. Unexpectedly, this approach revealed facultative incorporation of selenium as selenocysteine or selenomethionine into proteins that lack canonical encoding for selenocysteine. Selenium was selectively incorporated into regulatory sites on key metabolic proteins, including as selenocysteine-replacing cysteine at position 253 in uncoupling protein 1 (UCP1). This facultative utilization of selenium was initiated by increasing cellular levels of organic, but not inorganic, forms of selenium. Remarkably, dietary selenium supplementation elevated facultative incorporation into UCP1, elevated energy expenditure through thermogenic adipose tissue, and protected against obesity. Together, these findings reveal the existence of facultative protein selenation, which correlates with impacts on thermogenic adipocyte function and presumably other biological processes as well.

ROS | cysteine | selenocysteine | brown adipose tissue

Thermogenesis in brown and beige adipose tissues can combat obesity and diabetes, encouraging investigation of mechanisms that control this process. Recently, interventions that modify physiological reactive oxygen species (ROS) levels in brown adipose tissue (BAT) and beige fat have illustrated an important role for redox signaling in thermogenesis in vivo (1–4). Redox signaling by ROS drives activation of thermogenic gene programs (2), potentiates thermogenic respiration (1–3), and involves oxidative modification of sensitive cysteine (Cys) thiol residues on protein targets (1–3). Selenocysteine (Sec) is one of the rarest proteogenic amino acids and differs from Cys by a single atom, containing selenium instead of sulfur on its side chain. This difference renders Sec much more reactive due to a lower side-chain pK_a and stronger nucleophilicity compared to Cys (5). Sec incorporation into proteins is thought to be limited to the so-called selenoproteins, the 24 to 25 proteins (depending on species) in mammals, in which Sec is exclusively encoded at a particular site by cotranslational *cis*- and *trans*-acting elements (6). In this small number of mammalian selenoproteins, Sec typically exists in enzyme active sites to facilitate catalytic redox reactions. The physiological action of these selenoproteins depends strictly on the presence of Sec, with mutagenesis to Cys leading to decreased or abrogated functionality (6). The existence of currently identified selenoproteins is accounted for by nucleotide sequence analysis of cotranslational *cis* elements.

Because of the enhanced redox sensitivity encoded by Sec, and the importance of redox signaling in adipose tissue thermogenesis, we investigated whether selenoprotein status modifies thermogenic function in BAT. To begin examining this possibility, we first developed a targeted mass spectrometry (MS) approach to identify selenium insertion into proteins. In addition to identifying well-established obligate selenoproteins, this approach unexpectedly revealed heterogeneous but nonrandom incorporation of selenocysteine and selenomethionine into other proteins. We term these newly found selenation events "facultative," as they do not represent the cognate amino acid position in the entire pool of individual proteins and are not required for basic protein functionality. We found that selenation of these facultative sites increases in response to elevating selenomethionine levels. Sites where this heterogeneous incorporation was observed included the regulatory amino acid 253 of UCP1, which until now has only been observed as a Cys and is a major effector of adipose tissue thermogenesis. This unexpected evidence of Sec incorporation into UCP1 was indicative of a distinct pool of protein rendered exquisitely sensitive to redox modification, more so than the corresponding cysteine form. Moreover,

Significance

Oxidation of cysteines by reactive oxygen species (ROS) initiates thermogenesis in brown and beige adipose tissues. Cellular selenols, where selenium replaces sulfur, exhibit enhanced reactivity with ROS. Here we developed a mass spectrometric method to interrogate incorporation of selenols into proteins. Unexpectedly, this approach revealed facultative incorporation of selenium into proteins that lack canonical encoding for selenocysteine. Selenium was selectively incorporated into regulatory sites on key metabolic proteins, including as selenocysteine replacing cysteine at position 253 in UCP1 uncoupling protein 1 (UCP1). Remarkably, dietary selenium supplementation elevated facultative incorporation into UCP1, elevated energy expenditure through thermogenic adipose tissue, and protected against obesity. Together, these findings reveal the existence of facultative protein selenation, which correlates with effects on thermogenic adipocyte function.

Author contributions: M.P.M., V.N.G., S.P.G., E.T.C., and B.M.S. designed research; M.P.J., G.Z.L., J.S., M.M., R.G., J.A.P., D.K.S., D.L.-B., and L.K. performed research; and M.P.J., E.T.C., and B.M.S. wrote the paper.

Reviewers: D.J.M., University of Texas Southwestern Medical Center; and L.A.S., University of Hawaii at Manoa.

The authors declare no competing interest.

Data deposition: Data are available via ProteomeXchange with identifier PXD018225.

[1]To whom correspondence may be addressed. Email: Mark_Jedrychowski@hms.harvard.edu, EdwardT_Chouchani@dfci.harvard.edu, or Bruce_Spiegelman@dfci.harvard.edu.

This article contains supporting information online at https://www.pnas.org/lookup/suppl/doi:10.1073/pnas.2001387117/-/DCSupplemental.

First published May 1, 2020.

we found that increasing protein selenation through increased dietary selenium coincided with significant elevation in whole-body energy expenditure driven by thermogenic adipose tissue, and protection from obesity.

Results

Mass Spectrometric Method for Identification of Selenocysteine-Containing Proteins. Our recent examinations of redox regulation of adipose tissue thermogenesis have relied on the use of quantitative MS to identify redox-sensitive regulatory cysteine residues (1). Sec enhances protein redox sensitivity, but the role of selenium status in thermogenesis has not been systematically investigated. Although systematic methods for assessment of Sec-containing peptides by MS have not been widely employed, recent studies have shown that these species should be amenable to detection using standard peptide preparations, and that selenium could potentially be more broadly incorporated into proteins than previously appreciated (7, 8). To test this, we analyzed the mouse brown fat proteome for modifications corresponding to the mass of Sec. As expected, this approach successfully identified peptides corresponding to well-established selenoproteins (e.g., glutathione peroxidase 1 [Gpx1]; *SI Appendix*, Fig. S1 *A–C*). Unexpectedly, we also identified a number of peptides predicted to contain a Cys with additional mass corresponding exactly to the mass difference between Cys and Sec. An example of this was identified on the UCP1 tryptic peptide containing Cys253, which was identified as a second form shifted in mass by +47.94445 Da (Fig. 1*A*). This mass shift was observed exclusively for the Cys253 peptide and was never observed in the other six UCP1 tryptic peptides containing Cys (*SI Appendix*, Fig. S2). This intriguing finding led us to examine if a portion of the total pool of UCP1 and other proteins may facultatively incorporate Sec at particular Cys sites.

We first developed a targeted-MS approach for determination of Sec-containing peptides. Like Cys, Sec reacts efficiently and irreversibly with thiol derivatizing agents, such as *N*-ethylmaleimide (NEM) and iodoacetamide (IAM), which are typically used in redox-proteomic workflows (9). Therefore, in principle, Sec-containing peptides can be readily identified by a distinct mass shift corresponding to the mass of Sec + the covalent conjugate of the derivatizing agent (9, 10). Importantly, selenium exhibits a distribution of naturally occurring stable isotopes not found in any other element. In addition to the most abundant isotope, ^{80}Se (~50% total), four other stable isotopes exhibit sufficient natural abundance to be distinguished by MS, thus generating a unique isotopic signature (*SI Appendix*, Fig. S1*A*). Therefore, a peptide containing bona fide cysteine-to-selenocysteine replacement exhibits the following distinct features upon MS analysis. They must have a fragment spectrum mass attributable to Sec at a Cys locus (Fig. 1*B*, *Bottom*) that can be shifted in mass by derivatization with Sec-reactive nucleophiles to the mass of Sec + the derivatizing agent (Fig. 1*B*, *Middle*). Additionally, this peptide must exhibit the unique Sec mass isotope fingerprint (Fig. 1*B*, *Top*).

We first validated the analytic framework described above by MS analysis of Gpx1, a classic selenoprotein that is abundant in mouse BAT. As expected, we readily identified the Gpx1 Sec site by a unique mass shift and fragment spectrum attributable to Sec derivatization with NEM (*SI Appendix*, Fig. S1*A*). The expected Sec mass isotope fingerprint was also observed (*SI Appendix*, Fig. S1*A*). We next applied this approach to targeted MS profiling of BAT UCP1. MS identified UCP1 peptides containing six of seven UCP1 cysteine residues in the protein following derivatization with NEM (*SI Appendix*, Fig. S2). Uniquely, a UCP1-Sec253 peptide was identified that exhibited the molecular features unique to Sec-containing tryptic peptides. The major precursor ion mass corresponded to Sec alkylated with NEM (Fig. 1*C*), indicating Sec derivatization. Moreover, this precursor peptide mass exhibited the unique selenium isotope fingerprint (Fig. 1*C*). Additionally, high-accuracy peptide fragment ions demonstrated that the Sec mass addition was localized to position 253 (Fig. 1*D*). As the UCP1 peptide spanning position 253 contains two methionines, the form of this peptide containing oxidized methionines can also be present. We additionally identified the UCP1-Sec253 peptide in the methionine oxidized form. This peptide also exhibited all key unique features of a Sec replacement of Cys (Fig. 1 *E* and *F*). Notably, none of the Sec-specific features described for these peptides were present in the Cys form of the UCP1-253 peptide (*SI Appendix*, Fig. S2).

Validation and Quantification of UCP1-Sec253. To confirm the identity of the putative UCP1 selenium-containing peptide, we generated a synthetic peptide identical to the endogenous UCP1 Cys253 peptide with a selenocysteine replacement at position 253 and an isotopically heavy tyrosine (AQUA [Absolute Quantification] peptide + 10.0272 Da; *SI Appendix*, Fig. S3 *A* and *B*). This molecule allows for both identification and quantification of the endogenous selenated peptide. To determine the presence of UCP1 Sec253 in the brown fat proteome, the AQUA standard was derivatized with a distinct isobaric tandem mass tag (TMT) reporter. In this way the AQUA peptide allows for endogenous peptide identification by multiplexing (*SI Appendix*, Fig. S3*D*). We found that the endogenous UCP1 peptide displayed physiochemical properties identical to the AQUA standard, confirming the presence of Sec in position 253 of UCP1 (*SI Appendix*, Fig. S3*D*).

Use of the AQUA internal standard allowed estimation of the stoichiometry of the selenation replacement of cysteine at position 253. We examined the stoichiometry of selenation in BAT of wild-type (WT) male mice under standard housing conditions. In this case, selenium incorporation was estimated at ~4–5% of the total UCP1 protein (Fig. 2*A*). Thus, under these conditions it appears that a small but substantial proportion of UCP1 exists in selenated form.

We previously found that UCP1 Cys253 thiol can become oxidatively modified to a sulfenic acid upon activation of thermogenesis in vivo, a physiological stimulus that increases ROS levels in BAT. Moreover, based on mutagenesis and pharmacological manipulation of this residue, modification of this site is sufficient to affect UCP1 function. Sec exhibits extraordinary sensitivity to oxidative modification compared to Cys, so we examined whether selenated UCP1 was more sensitive to oxidative modification. Remarkably, we found that, under baseline conditions when Cys253 is predominantly unmodified, Sec253 is substantially oxidized to a selenenic acid (Fig. 2*B*). Therefore, the Sec253 form of UCP1 represents a substantial and distinct pool of the protein that is highly sensitive to oxidation.

Facultative Incorporation of Selenium into Proteins Occurs via a Noncanonical Pathway. We next examined how selenium could be incorporated into proteins such as UCP1, whose sequence contains no apparent coding for Sec incorporation via established cotranslational pathways. Cotranslational incorporation of selenium as Sec is facilitated by a distinct transfer RNA (tRNA) charging mechanism that utilizes inorganic selenite as the source for selenium. In addition, organic forms of selenium can contribute to this cotranslational pathway via the release of selenide or its derivatives. This mode of incorporation can be observed by protein autoradiography following supplementation with ^{75}Se-selenite. ^{75}Se-selenite–treated brown adipocytes exhibited robust labeling of proteins with molecular masses corresponding to well-established selenoproteins, but no signal was observed at the molecular mass corresponding to UCP1 (Fig. 2*C*). Despite this, Sec253 incorporation in UCP1 was readily apparent by MS of the brown adipocyte protein, suggesting that facultative Sec incorporation occurs independent of this cotranslational pathway.

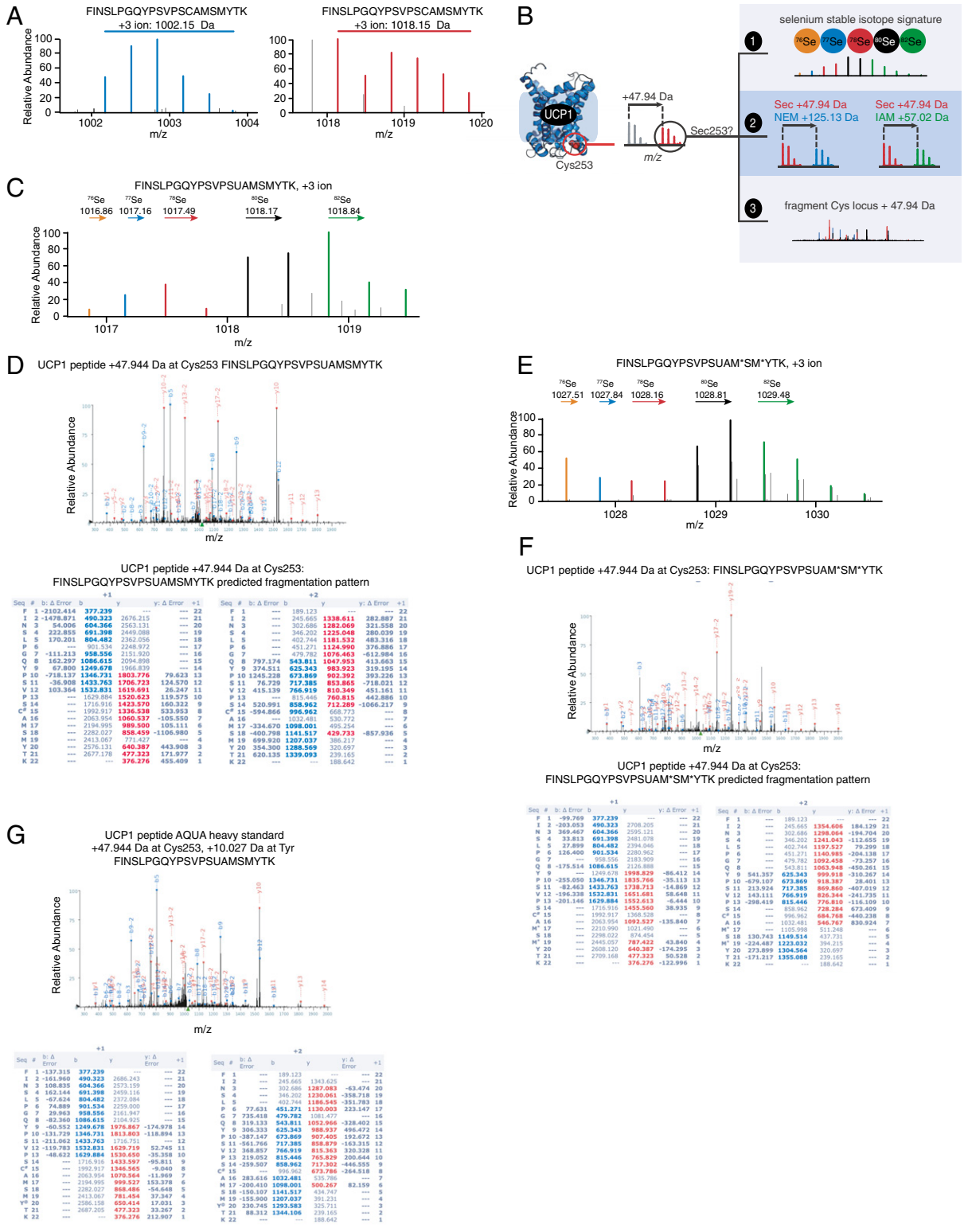

Fig. 1. Selenocysteine incorporation into 253 locus of UCP1. (*A*) MS1 spectrum of UCP1 tryptic peptide spanning position 253 with a mass shift corresponding to the exact mass difference between cysteine and selenocysteine. This peptide is +3, so the *m/z* shift indicates a mass difference of 47.94 Da. (*B*) MS criteria for identification of a facultative selenocysteine site; (*Top*) presence of MS1 selenium isotope signature; (*Middle*) mass shift corresponding to addition of selenocysteine derivatization agents; (*Bottom*) fragment mass spectrum localizing selenium mass to cysteine locus. (*C*) Presence of selenium stable isotope signature on mass-shifted UCP1 peptide spanning position 253. Colors indicate peaks matching the stable isotope signature of selenium shown in *B*. (*D*) Fragment spectrum of UCP1 peptide localizing the mass difference between sulfur and selenium to position 253. (*E*) Presence of selenium stable isotope signature on methionine-oxidized form of mass-shifted UCP1 peptide spanning position 253. Colors indicate peaks matching the stable isotope signature of selenium shown in *B*. (*F*) Fragment spectrum of UCP1 methionine-oxidized peptide localizing the mass difference between sulfur and selenium to position 253. (*G*) Fragment spectrum of synthetic AQUA peptide with selenocysteine at position 253.

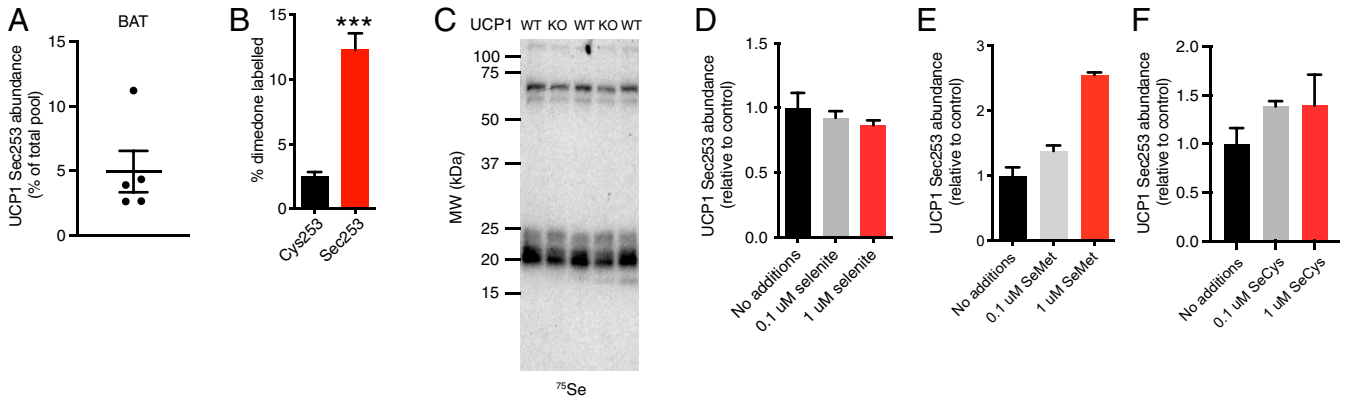

Fig. 2. Characterization of selenocysteine incorporation into the UCP1 253 locus. (*A*) Proportion of selenocysteine 253 form of UCP1 estimated using internal standard AQUA peptides. (*B*) Relative abundance of selenenic acid and sulfenic acid forms of UCP1; $n = 3$. (*C*) Autoradiogram of WT and UCP1KO brown adipocyte lysates treated with sodium ^{75}Se-selenite throughout differentiation. Prominent band in the 20- to 25-kDa region indicates well-established GPx selenoprotein family. No observable signal in the molecular weight (MW) region of UCP1 (~33 kDa). (*D*) Relative changes in content of the selenocysteine form of UCP1 in brown adipocytes treated with sodium selenite; $n = 3$. (*E*) Relative changes in content of the selenocysteine form of UCP1 in brown adipocytes treated with selenomethionine; $n = 3$. (*F*) Relative changes in content of the selenocysteine form of UCP1 in brown adipocytes treated with selenocysteine (SeCys); $n = 3$.

To test this further, we treated primary brown adipocytes with increasing concentrations of sodium selenite throughout differentiation, when UCP1 protein is generated de novo at high levels. As expected, sodium selenite increased the abundance of classical selenoproteins for which Sec incorporation occurs cotranslationally (*SI Appendix*, Fig. S3*E*). However, under these conditions sodium selenite had no effect on the levels of UCP1-Sec253 (Fig. 2*D*). We next considered whether other forms of selenium may contribute to facultative incorporation into proteins. Organic forms of selenium are a major source of selenium and can be generated from selenite via systemic metabolism by microbes and many other organisms. Among the most prevalent forms of organic selenium is selenomethionine. When brown adipocytes were supplemented with selenomethionine throughout differentiation, the proportion of the Sec253 form of UCP1 increased substantially (Fig. 2*E*). Interestingly, this was not observed when cells were supplemented with the other major organic form of selenium, selenocysteine (in the form of selenocystine, which is the oxidized form of selenocysteine) (Fig. 2*F*).

Importantly, the tryptic peptide of UCP1 that contains Sec253 also contains two methionines. Therefore, the observed increase in selenation of this peptide following selenomethionine treatment could be attributable to selenomethionine incorporation instead of selenocysteine. To distinguish between these two possibilities, we examined the fragment spectra of the selenated UCP1 tryptic peptide. By examining the b and y ions spanning the Cys and Met locus, we found that the selenium addition was attributable exclusively to position 253 (Fig. 1 *D–G* and *SI Appendix*, Fig. S3*E*).

Dietary Selenium Supplementation Modifies Both Obligate and Facultative Selenoproteins but at Different Dietary Concentrations. Modulation of the classic selenoproteins can be readily achieved by dietary supplementation of sodium selenite (11). Dietary selenite is assimilated from the diet and converted by endogenous metabolism to generate organic selenium-containing metabolites including selenomethionine and selenocysteine. The mechanisms through which this occurs are not clear, but appear to involve utilization by multiple tissues, including the liver and gut. Interestingly, there is evidence that dietary selenium status may play a role in modulating energy homeostasis, but the mechanisms that underlie this are unclear (12, 13). Moreover, there has been no systematic determination of selenium incorporation into adipose tissue proteins following modulation of dietary selenium. We therefore made use of diets containing defined amounts of selenite to investigate this (11). A selenium-deficient diet (<0.03-ppm selenium) is below the minimal threshold to generate basal levels of obligate selenoproteins. Selenium at 0.1 ppm corresponds to the daily recommended intake of selenite and the minimal amount required to achieve maximal expression of obligate selenoproteins (11, 14). Selenite at 0.4 ppm corresponds to the common dose used in human clinical studies (11, 15), and 2.25-ppm selenite corresponds to a safe high level well above the amount required for maximal obligate selenoprotein synthesis (11). Diets were provided to mice for 8 wk prior to isolation of BAT and analysis by MS.

As expected, we found that expression of obligate selenoproteins in BAT depended on dietary selenite and that expression was saturated by dietary supplementation between 0.1-and 0.4-ppm selenite (Fig. 3*A*). We additionally used MS to examine the breadth of facultative selenium incorporation across the BAT proteome. Using the criteria described in Fig. 1*B*, we observed several apparent facultative Sec sites (Fig. 3*B*). Our findings suggest that selenium is incorporated more broadly into proteins than previously appreciated. Remarkably, across four biological replicate experiments facultative protein selenation was highly specific to certain residues, indicating nonrandom incorporation. Most of these sites were localized within core metabolic proteins such as aconitase, malate dehydrogenase, and fatty acid synthase (Fig. 3*B*). Notably, some of these sites have established functional roles in controlling protein function. For example, cysteine 451 in mitochondrial aconitase is critical for Fe-S coordination and enzymatic activity, and is known to be subject to redox modification (16). Numerous other sites are not known to be sites of redox regulation, but the reproducible and specific facultative selenation signature suggests that these sites may be previously unappreciated regulatory sites.

We also identified numerous instances of selective, nonrandom incorporation of selenium as selenomethionine into methionine-encoding loci (Fig. 3*C*). The majority of targets of selenomethionine insertion were also major metabolic enzymes and fatty acid–handling proteins. Moreover, some proteins, such as fatty acid-binding protein 4, exhibited separate instances of selenocysteine and selenomethionine incorporation (Fig. 3 *B* and *C*). In parallel, we examined subcutaneous white adipose tissue for the presence of facultative selenomethionine and selenocysteine sites. We identified one facultative selenocysteine site and

A

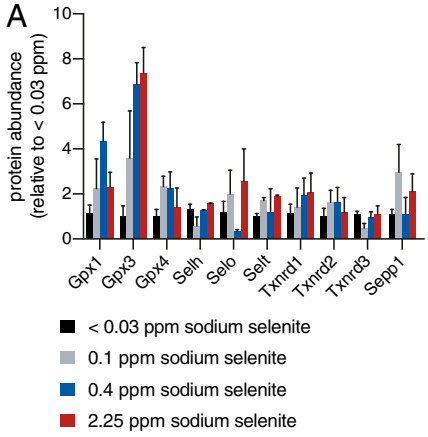

B

protein	peptide	locus
UCP1	R.FINSLPGQYPSVPSC#AM*SM*YTK.E	253
ACON	R.DVGGIVLANACGPC#IGQWDR.K	451
FAS	K.STLATSSSQPVWLTAMDC#PTSGVVGLVNCLR.K	1440
ECHA	K.EVESVTPEHC#IFASNTSALPINQIAAVSK.R	471
TKT	K.QAFTDVATGSLGQGLGAAC#GM*AYTGK.Y	132
KALRN	K.AEQFLSGVDAWC#K.M	417
SAE1	K.VLFC#PVK.E	218
GWL	R.DC#QVSSK.Y	325
PPIF	R.VIPAFMC#QAGDFTNHNGTGGR.S	104
FABP4	R.DGDKLVVEC#VMK.G	218
ETFB	K.QAIDDDC#NQTGQMTAGLLDWPQGTFASQVTLEGDK.V	131
ACACA	K.IIEEAPAAIATPAVFEHMEQC#AVK.L	406
ACADM	R.MTEQPMMC#AYCVTEPSAGSDVAAIK.T	156
KPYM	R.AEGSDVANAVLDGADC#IM*LSGETAK.G	358
ALBU	K.DDNPSLPPFERPEAEAM#C#TSFK.E	47

C

protein	peptide	locus
IDH3G	NIANPTATLLASCM#M#LDHLK	334/335
CO5A2	R.GPQGLQGQQGGVGPAGPPGEPGEPGPM#GPIGSR.G	246
GPDA	R.LGIPM#SVLMGANIASEVAEEK.F	144
THIM	K.DM#DLIDVNEAFAPQFLSVQK.A	314
PSMD2	R.QLM#SQVAVAGLLTVLVSFLDVR.N	788
LDHA	K.DLADELALVDVM#EDK.L	54
KPYM	R.AEGSDVANAVLDGADC#IM#LSGETAK.G	360
ALBU	K.DDNPSLPPFERPEAEAM#C#TSFK.E	47
1433E	R.DNLTLWTSDM#QGDGEEQNK.E	235
TBB4A	K.M#AATFIGNSTAIQELFK.R	363
GPDA	R.VTM#WVFEEDIGGR.K	38
GSTP2	R.EAAQVDM#VNDGVEDLR.G	92
FABP4	K.LVSSENFDDYM#K.E	21
PGK1	K.TGQATVASGIPAGWM#GLDCGTESSK.K	312
FUMH	K.LNDHFPLVVWQTGSGTQTNM#NVNEVISNR.A	147
CISY	R.LDWSHNFTNM#LGYTDPQFTELMR.L	243
NDUAC	K.NTFWDVDGSM#VPPEWHR.W	81

D

protein	peptide	locus
PDHA2	NFYGGNGIVGAQVPLGAGVAFAC#K	182
GSTP2	EAAQVDM#VNDGVEDLR	92

E

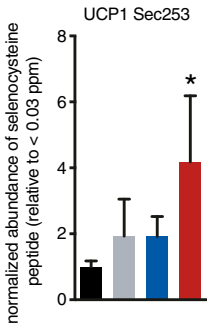

Fig. 3. Dietary selenium differentially modifies canonical and facultative selenation of proteins. (*A*) Expression of canonical selenoproteins mapped in this study of BAT and modulated by 0.1- to 0.4-ppm dietary sodium selenite; $n = 5$. (*B*) Identification of selective facultative selenocysteine insertion into BAT metabolic proteins; $n = 5$. (*C*) Identification of selective facultative selenomethionine insertion into BAT metabolic proteins; $n = 5$. (*D*) Identification of selective facultative selenomethionine and selenocysteine insertion into s.c. white adipose tissue proteins; $n = 5$. (*E*) 2.25-ppm dietary selenium increases the amount of Sec253 UCP1; $n = 5$.

one selenomethionine site (Fig. 3*D*). We next investigated whether transcripts encoding proteins that contain facultative selenocysteine and selenomethionine sites exhibited any structural features suggestive of cotranslational regulatory elements.

Genomic Features of Genes Encoding Proteins with Facultative Selenation. We next investigated whether transcripts encoding proteins that contain facultative selenocysteine and selenomethionine sites exhibited any structural features suggestive of the selenation mechanism. First, we searched for potential SECIS (selenocysteine insertion sequence) elements. We scanned gene sequences with SECISearch3 (17) with default parameters, which returned no SECIS hit. We thus ran an extended search with maximum sensitivity settings, and identified a number of potential candidates. We analyzed them for the presence of known functional features of SECIS, which led to dismissal of the majority of candidates (*SI Appendix*, Fig. S4). Only one gene encoding a protein with facultative selenomethionine (26S proteasome non-ATPase regulatory subunit 2 [PSMD2]) and one with facultative selenocysteine (GWL) contain potentially functional SECIS elements. Based on their sparse occurrence and inconsistent positioning within gene structures (*SI Appendix*, Fig. S5), SECIS elements are likely not relevant to the facultative selenation mechanism. Next, we explored the possibility of other cotranslational regulatory elements, searching these genes for any RNA structures conserved across mammals. While we identified a number of candidate structures, we found no common motifs across structures in different genes, suggesting no link with selenation. Analogously, the search for peptide motifs in proteins with facultative selenation found no significantly enriched sequence pattern. We noted, however, that proteins with facultative selenation are involved in recurrent biological pathways. Indeed, our analysis identified a number of significantly enriched functional annotations (*SI Appendix*, Table S1), including various metabolic processes, and localization to mitochondria and exosomes.

Dietary Selenium Status Regulates Adipose Tissue Thermogenesis and Modifies Obesogenesis. Notably, between 0.1- and 0.4-ppm dietary selenium was sufficient to maximize classical selenoprotein expression in BAT. However, through quantification of UCP1-Sec253 we found selenation of this site was elevated only by 2.25-ppm selenite (Fig. 3*E*). Therefore, the threshold for obligate selenoprotein synthesis and facultative selenation of UCP1 appear to be distinct.

Based on our analysis of adipose tissue protein selenation following dietary selenium modification, we were able to distinguish between the following physiological states: 1) low total protein selenation with low levels of obligate selenoproteins and low facultative UCP1 selenation driven by <0.03-ppm dietary selenium (Fig. 3 *A* and *C*); 2) high levels of obligate selenoproteins and low levels of facultative UCP1 selenation driven by 0.1- to 0.4-ppm dietary selenium (Fig. 3 *A* and *C*); 3) high levels of obligate selenoproteins and high levels of facultative UCP1 selenation driven by 2.25-ppm dietary selenium (Fig. 3 *A* and *C*). Under these conditions, we examined whether modification of obligate or facultative selenium status affects metabolic physiology regulated by thermogenic adipose tissue.

Following 8-wk supplementation with defined selenium diets (Fig. 4 *A–C*), mice were subjected to acute pharmacological stimulation of BAT and beige adipose tissue thermogenesis using the β3-agonist CL-316 243 (CL; Fig. 4 *D–F*). Importantly, mice on the 2.25-ppm selenium diet exhibited enhanced β3-adrenoreceptor–stimulated oxygen consumption and CO_2 release compared to all other groups (Fig. 4 *D–F*). Interestingly, no difference in energy expenditure was observed between the selenium-depleted group and 0.1-ppm and 0.4-ppm supplemented groups (Fig. 4 *D–F*). Together, these data suggest that modification of obligate selenoprotein status does not affect BAT and beige thermogenesis. However, further elevation of selenium status at 2.25 ppm, which coincides with elevated facultative UCP1 selenation, enhances thermogenesis (Fig. 4 *A–F*).

Since elevating dietary selenium was sufficient to potentiate BAT thermogenesis by β3-adrenoreceptor agonism, we explored whether this intervention could modify the physiological response to high-fat feeding. We compared 1) mice ingesting a high-fat diet (HFD) supplemented with 0.1-ppm dietary selenium, a level sufficient for expression of selenoproteins in BAT (Fig. 3*A*) and having no effect on BAT thermogenesis (Fig. 4 *D–F*); and 2) mice ingesting an HFD supplemented with 2.25-ppm dietary selenium, a level sufficient to elevate facultative UCP1 selenation in BAT (Fig. 3*C*) and stimulate BAT thermogenesis (Fig. 4 *D–F*). As shown in Fig. 4 *G* and *H*, mice on 2.25-ppm selenium diets exhibited robust protection against weight gain upon high-fat feeding over 14 wk. Moreover, this effect was specifically attributable to a decrease in fat mass (Fig. 4*I*). Notably, this protection against obesity occurred despite there being no detectable changes in food intake (Fig. 4*J*), and absent elevation in liver inflammation or fibrosis (Fig. 4*K* and *SI Appendix*, Fig. S6).

Discussion

In humans, elevated dietary selenium intake has been linked to protection against obesity and diabetes (12, 13), although the underlying mechanisms remain unknown. Because of the established role of selenium as a regulator of redox and ROS metabolism, here we systematically investigated its role in regulating thermogenic adipose tissue function in mice. Remarkably, we found that modification of selenium status has robust and substantial effects on energy expenditure and adipose tissue thermogenesis. These effects coincide with previously unappreciated modes of selenium use in thermogenic adipose tissue. Specifically, we showed that selenium is selectively encoded into cysteine and methionine sites of a class of facultative (as opposed to obligate) selenoproteins. While the mechanism of facultative selenation remains unclear, it occurs in nonrandom fashion in proteins involved in specific pathways, prominently metabolic processes, suggesting that this phenomenon may have a biological function. Importantly, nonrandom incorporation is observed in the case of both selenocysteine and selenomethionine, suggesting that both events mark protein regulatory sites. The exemplar is UCP1, which we showed can incorporate Sec at position 253 as an alternative to Cys. We also demonstrated that UCP1-Sec253 is highly sensitive to redox modification, and that increasing the pool of this type of facultative selenoprotein coincides with BAT-dependent energy expenditure in vivo. The high propensity for UCP1-Sec253 to be oxidatively modified may be indicative of a pool of UCP1 that is highly sensitive to activation by elevated ROS, as observed in previous studies. It is therefore also possible that physiological effects attributable to shifts in dietary selenium are mediated by facultative protein selenation on these proteins. It is worth noting that, in brown adipocytes, selenomethionine can increase facultative selenation of UCP1 but selenocysteine cannot. This suggests privileged access of the selenium in selenomethionine to the facultative protein selenation pathway. In addition to UCP1, other major metabolic proteins display signatures indicative of selenation at either cysteine or methionine. It is therefore likely that physiological effects attributable to facultative protein selenation occur in response to modification of many of these proteins.

Taken together, these findings suggest a noncanonical paradigm for encoding enhanced redox sensitivity and functionality in proteins. Moreover, they demonstrate that modification of selenium status in the diet may be a relatively simple means of enhancing thermogenic function in adipose tissues and modifying obesity in humans.

Methods

Animal Experiments. Animal experiments were performed as described previously (3), according to procedures approved by the Institutional Animal Care and Use Committee of the Beth Israel Deaconess Medical Center. Mice were male C57BL/6J (age 12 wk; Jackson Laboratories) and were housed in a temperature-controlled (23 °C) room on a 12-h light–dark cycle.

Primary Brown Adipocyte Preparation and Differentiation. Interscapular brown adipose stromal vascular fraction was obtained as described previously (3).

Sample Preparation for Mass Spectrometry. Samples were homogenized in 50-mM Tris base containing 100-mM NaCl, 100-μM diethylenetriamine pentaacetate (DTPA), 0.1% sodium dodecyl sulfate (SDS), 0.5% sodium deoxycholate, 0.5% Triton X-100, 10-mM tris(2-carboxyethyl)phosphine (TCEP), and 50-mM iodoacetamide or 50-mM NEM depending on the experiment. Following incubation for 15 min, SDS was added to a final concentration of 1% and samples were incubated for a further 15 min.

Protein Digestion. Protein pellets were dried and resuspended in 8-M urea containing 50-mM Hepes (pH 8.5). Protein concentrations were measured by bicinchoninic acid assay (ThermoFisher Scientific) before protease digestion. Protein lysates were diluted to 4-M urea and digested with LysC (Wako, Japan) in a 1/100 enzyme/protein ratio overnight. Protein extracts were diluted further to a 1.0-M urea concentration, and trypsin (Promega) was added to a final 1/200 enzyme/protein ratio for 6 h at 37 °C. Digests were acidified with 20-μL 20% formic acid (FA) to a pH ~2, and subjected to C18 solid-phase extraction (50-mg SepPak, Waters).

LC–MS/MS Parameters for Peptide Analysis. All spectra were acquired using an Orbitrap Fusion mass spectrometer (ThermoFisher Scientific) in line with an Easy nLC 1000 (ThermoFisher Scientific) ultrahigh-pressure liquid chromatography (LC) pump as described previously (3, 18).

Assessment of Protein Thiol Sulfenic Acids. BAT was prepared adapting a protocol used previously to stabilize endogenous protein sulfenic acids (18). Briefly, samples were homogenized in 50-mM Tris base containing 100-mM NaCl, 100-μM DTPA, 0.1% SDS, 0.5% sodium deoxycholate, 0.5% Triton-X 100, and 5-mM dimedone. To minimize lysis-dependent oxidation, buffers

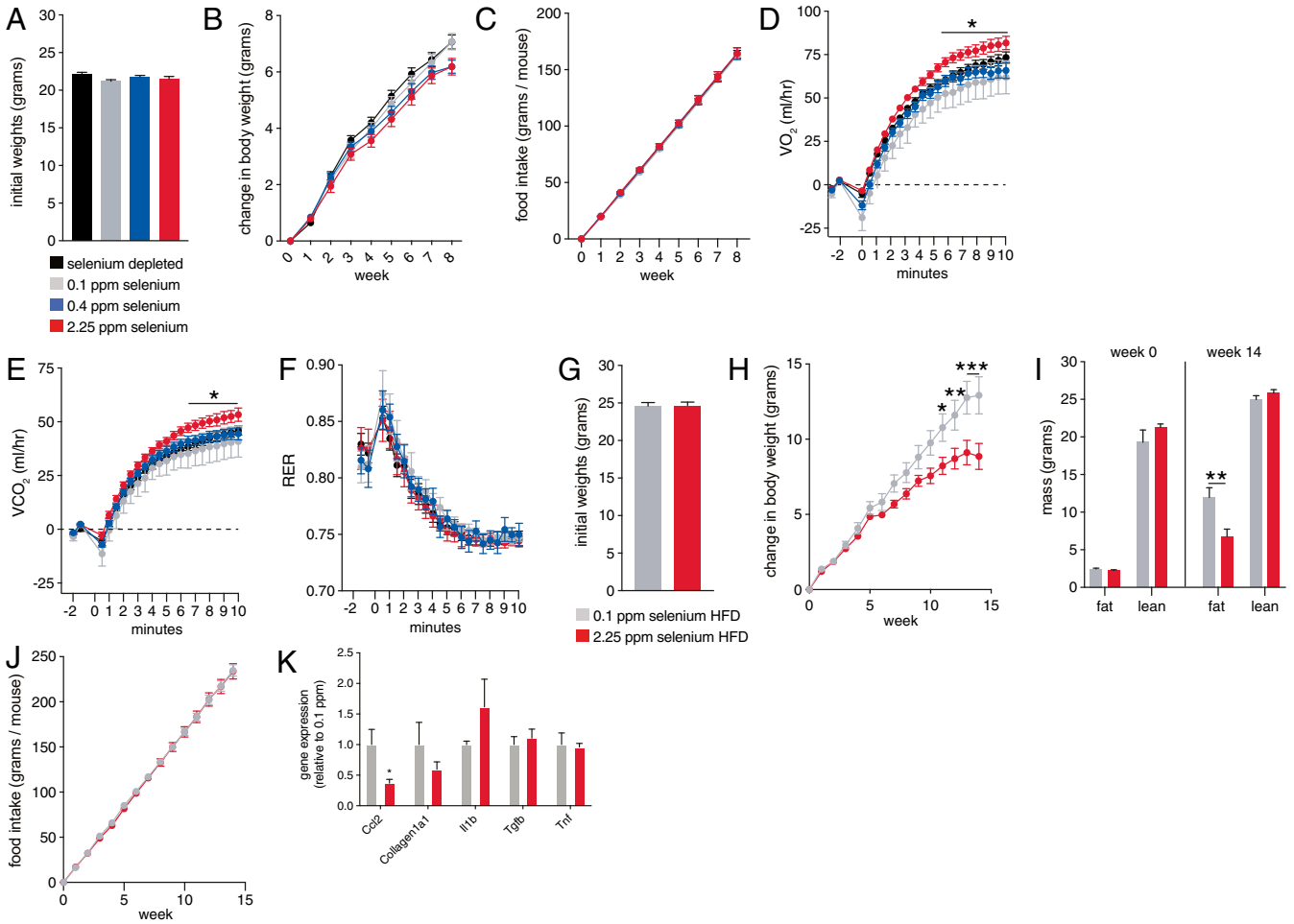

Fig. 4. Elevated dietary selenium enhances BAT energy expenditure and protects against obesogenesis induced by high-fat feeding. (*A*) Weight of mice prior to intervention with defined selenium-containing chow diets; $n = 24$ to 25. (*B*) Weight gain of mice on chow diets containing defined selenium concentrations; $n = 24$ to 25. (*C*) Cumulative food intake of mice on chow diets containing defined selenium concentrations; $n = 24$ to 25. (*D*) Whole-body oxygen consumption upon acute 1-mg/kg CL of mice following 8 wk on chow diets containing defined selenium concentrations; $n = 7$. (*E*) Whole-body CO_2 release upon acute 1-mg/kg CL of mice following 8 wk on chow diets containing defined selenium concentrations; $n = 7$. (*F*) Whole-body respiratory exchange quotient (RER) upon acute 1-mg/kg CL of mice following 8 wk on chow diets containing defined selenium concentrations; $n = 7$. (*G*) Weight of mice prior to intervention with defined selenium-containing HFD; $n = 12$ to 15. (*H*) Weight gain of mice on HFD containing 0.1- or 2.25-ppm sodium selenite; $n = 12$ to 15. (*I*) Whole-body composition of mice following 8 wk HFD containing either 0.1- or 2.25-ppm sodium selenite; $n = 12$ to 15. (*J*) Cumulative food intake of mice on HFD containing either 0.1- or 2.25-ppm sodium selenite; $n = 12$ to 15. (*K*) Liver fibrosis and inflammation markers of mice on HFD containing either 0.1- or 2.25-ppm sodium selenite; $n = 4$.

were bubbled with argon before use. Samples were incubated for 15 min at room temperature, at which point SDS was added to a final concentration of 1% and samples were incubated for a further 15 min. After dimedone treatment, 10-mM TCEP and 50-mM NEM were added and samples were incubated for a further 15 min at 37 °C to reduce and alkylate all nonsulfenic acid protein cysteine residues. Samples were then subjected to protein digestion and LC-MS/MS as described above.

Determination of Peptides Containing Selenocysteine and Selenomethionine. A compendium of software developed in-house was used to convert mass spectrometric data (raw file) to the mzXML format, as well as to correct monoisotopic mass-to-charge ratio (*m/z*) measurements (19). All experiments used the Mouse UniProt database (downloaded March 2019), where reversed protein sequences and known contaminants such as human keratins were appended. SEQUEST searches were performed using a 50-ppm precursor ion tolerance, while requiring the peptide amino/carboxy (N/C) terminus to have trypsin protease specificity and allowing up to two missed cleavages. Ten-plex TMT tags on peptide N termini and lysine residues (+229.162932 Da) and carbamidomethylation (+57.02146 Da) or NEM (+125.047679) of cysteine residues were set as static modifications while methionine oxidation (+15.99492 Da) and selenium replaced sulfur (+47.9444) set as variable modifications. An MS^2 spectra assignment false discovery rate (FDR) of less than 1% was achieved by applying the target-decoy database search strategy (19). Filtering was performed using an in-house linear discrimination analysis (LDA) method to create one combined filter parameter from the following peptide ion and MS^2 spectra metrics: SEQUEST parameters XCorr and ΔCn, peptide ion mass accuracy and charge state, in-solution charge of peptide, peptide length, and miscleavages. Linear discrimination scores were used to assign probabilities to each MS^2 spectrum for being assigned correctly, and these probabilities were further used to filter the dataset with an MS^2 spectra assignment FDR of smaller than 1% at the protein level (20).

Quantification of UCP1 Sec253 Peptide Using Heavy Standard AQUA Peptides. The AQUA peptides employed in this study are as follows, where U* = selenocysteine and Y = heavy tyrosine 10.027228): AQUA peptide/sequence/mass (Da) Heavy; UCP1 240–261/FINSLPGQYPSVPSU*AMSMYTK/2477.20; and UCP1 240–261/FINSLPGQYPSVPSCAMSMYTK/2430.149.

Skyline version 19.1.0.193 was used to quantify absolute and relative amounts of UCP1 253 selenocysteine and cysteine in all experiments, with heavy AQUA peptides used as a reference (21).

Genomic Analyses of Facultatively Selenated Proteins. The mRNA sequences of genes encoding proteins with facultative selenation at cysteine or

methionine sites were scanned for the presence of SECIS elements using SECISearch3 (17). A first search with default parameters returned no results, so a subsequent run was performed activating all built-in search methods and deactivating the SECIS filter. Candidates were thus manually inspected and assessed considering the known functional features of SECIS (17). To search for any conserved RNA structure, whole-genome alignments encompassing 60 vertebrates were downloaded from ref. 22, and the regions corresponding to mRNAs of mouse genes with facultative selenation were extracted and searched with RNAz v2.1 (23). The coordinates of candidate RNA structures were plotted in respect to gene structures and selenation sites, and no consistent patterns across genes were found. Furthermore, the program MEME v5.1.0 (24) was used to assess the presence of significantly enriched nucleotide sequence motifs in the predicted RNA structures, considering the set of genes with selenation at cysteines or at methionines, or combining the two categories. We found no such motifs. We also used MEME in an analogous fashion to detect peptide motifs enriched in these genes, also with no results. Lastly, functional enrichment was assessed using DAVID (25). Three functional analyses were run, one for each of the gene sets (with selenation at cysteines, at methionines, or their union). In order to control for the gene expression profile of our cells, the lists of all genes with any (nonselenated) peptides detected in the same MS experiments were used as background to calculate enrichment. An FDR cutoff of 5% was applied.

Determination of Selenite Incorporation Using Sodium ^{75}Se-Selenite. Brown adipocytes were differentiated as described above. Freshly neutralized ^{75}Se-selenite was added to cells (5-mCi/mL medium) from day 0 and on each media change throughout differentiation to day 7. After labeling, cells were harvested, lysed, proteins quantified, and separated on SDS/polyacrylamide gel electrophoresis. The separated proteins were transferred onto polyvinylidene fluoride membranes and analyzed with a Typhoon PhosphorImager as described previously (26).

Sodium Selenite Dietary Intervention and High-Fat Feeding. All mouse dietary and high-fat feeding experiments were performed with age matched littermate controls. At age 8 wk, mice were switched to chow [Envigo 99256–selenium deficient (SD; 99257–0.1-ppm Se; 01390–0.4-ppm Se; 01391–2.25-ppm Se)] or high-fat diet (Envigo SD 170392; 2.25-ppm Se 170441) containing defined amounts of sodium selenite. Dietary intervention proceeded for 8 wk prior to molecular analyses.

Body Composition Analysis. Body composition was examined with Echo MRI (Echo Medical Systems) using the 3-in-1 Echo MRI Composition Analyzer.

Metabolic Phenotyping. Whole-body energy metabolism was evaluated using a Comprehensive Lab Animal Monitoring System (CLAMS; Columbia Instruments). CO_2 and O_2 levels were collected every 30 s. CL 316,243 (1 mg kg^{-1}; Sigma-Aldrich;) was injected intraperitoneally into mice at the indicated times.

Data Availability Statement. Data are available via ProteomeXchange with identifier PXD018225.

ACKNOWLEDGMENTS. The work was supported by the Claudia Adams Barr Program (to E.T.C. and M.P.J.), NIH Grant DK123095 (to E.T.C.), NIH Grants DK117149 and CA080946 (to V.N.G.), NIH Grant GM132129 (to J.A.P.), and the JPB Foundation (to B.M.S.).

1. E. T. Chouchani *et al*., Mitochondrial ROS regulate thermogenic energy expenditure and sulfenylation of UCP1. *Nature* **532**, 112–116 (2016).
2. Y. H. Han *et al*., Adipocyte-specific deletion of manganese superoxide dismutase protects from diet-induced obesity through increased mitochondrial uncoupling and biogenesis. *Diabetes* **65**, 2639–2651 (2016).
3. E. L. Mills *et al*., Accumulation of succinate controls activation of adipose tissue thermogenesis. *Nature* **560**, 102–106 (2018).
4. E. T. Chouchani, L. Kazak, B. M. Spiegelman, Mitochondrial reactive oxygen species and adipose tissue thermogenesis: Bridging physiology and mechanisms. *J. Biol. Chem.* **292**, 16810–16816 (2017).
5. D. L. Hatfield, P. A. Tsuji, B. A. Carlson, V. N. Gladyshev, Selenium and selenocysteine: Roles in cancer, health, and development. *Trends Biochem. Sci.* **39**, 112–120 (2014).
6. V. M. Labunskyy, D. L. Hatfield, V. N. Gladyshev, Selenoproteins: Molecular pathways and physiological roles. *Physiol. Rev.* **94**, 739–777 (2014).
7. D.W. Bak, J. Gao, C. Wang, E. Weerapana, A quantitative chemoproteomic platform to monitor selenocysteine reactivity within a complex proteome. *Cell Chem. Biol.* **25**, 1157–1167.e4 (2018).
8. L. Guo *et al*., Selenocysteine-specific mass spectrometry reveals tissue-distinct selenoproteomes and candidate selenoproteins. *Cell Chem. Biol.* **25**, 1380–1388.e4 (2018).
9. D. Fenyö, R. C. Beavis, Selenocysteine: Wherefore art thou? *J. Proteome Res.* **15**, 677–678 (2016).
10. E. Galano *et al*., Privileged incorporation of selenium as selenocysteine in *Lactobacillus reuteri* proteins demonstrated by selenium-specific imaging and proteomics. *Mol. Cell. Proteomics* **12**, 2196–2204 (2013).
11. S. V. Novoselov *et al*., Selenoprotein deficiency and high levels of selenium compounds can effectively inhibit hepatocarcinogenesis in transgenic mice. *Oncogene* **24**, 8003–8011 (2005).
12. Y. Wang *et al*., Significant beneficial association of high dietary selenium intake with reduced body fat in the CODING study. *Nutrients* **8**, 24 (2016).
13. Y. Wang *et al*., High dietary selenium intake is associated with less insulin resistance in the Newfoundland population. *PLoS One* **12**, e0174149 (2017).
14. R. F. Burk, Selenium, an antioxidant nutrient. *Nutr. Clin. Care* **5**, 75–79 (2002).
15. L. C. Clark *et al*., Effects of selenium supplementation for cancer prevention in patients with carcinoma of the skin. A randomized controlled trial. Nutritional Prevention of Cancer Study Group. *JAMA* **276**, 1957–1963 (1996).
16. N. Ternette *et al*., Inhibition of mitochondrial aconitase by succination in fumarate hydratase deficiency. *Cell Rep.* **3**, 689–700 (2013).
17. M. Mariotti, A. V. Lobanov, R. Guigo, V. N. Gladyshev, SECISearch3 and Seblastian: New tools for prediction of SECIS elements and selenoproteins. *Nucleic Acids Res.* **41**, e149 (2013).
18. C. Klomsiri *et al*., Use of dimedone-based chemical probes for sulfenic acid detection evaluation of conditions affecting probe incorporation into redox-sensitive proteins. *Methods Enzymol.* **473**, 77–94 (2010).
19. J. E. Elias, S. P. Gygi, Target-decoy search strategy for increased confidence in large-scale protein identifications by mass spectrometry. *Nat. Methods* **4**, 207–214 (2007).
20. E. L. Huttlin *et al*., A tissue-specific atlas of mouse protein phosphorylation and expression. *Cell* **143**, 1174–1189 (2010).
21. B. MacLean *et al*., Skyline: An open source document editor for creating and analyzing targeted proteomics experiments. *Bioinformatics* **26**, 966–968 (2010).
22. University of California, Santa Cruz, Data from "goldenPath." https://hgdownload.soe.ucsc.edu/goldenPath/mm10/multiz60way/. Accessed 21 January 2020.
23. A. R. Gruber, S. Findeiss, S. Washietl, I. L. Hofacker, P. F. Stadler, RNAz 2.0: Improved noncoding RNA detection. *Pac. Symp. Biocomput.* **15**, 69–79 (2010).
24. T. L. Bailey *et al*., MEME SUITE: Tools for motif discovery and searching. *Nucleic Acids Res.* **37**, W202–W208 (2009).
25. X. Jiao *et al*., DAVID-WS: A stateful web service to facilitate gene/protein list analysis. *Bioinformatics* **28**, 1805–1806 (2012).
26. S. H. Yim, R. Tobe, A. A. Turanov, B. A. Carlson, Radioactive ^{75}Se labeling and detection of selenoproteins. *Methods Mol. Biol.* **1661**, 177–192 (2018).